25th IMEKO TC4 International Symposium
23rd International Workshop on ADC and DAC Modelling and Testing
IMEKO TC-4 2022
Brescia, Italy / September 12-14, 2022

Image quality comparison of two different experimental setups for MEMS actuators functional evaluation: a preliminary study

Gabriele Bocchetta[1], Giorgia Fiori[2], Andrea Scorza[3], Salvatore Andrea Sciuto[4]

Dep. of Industrial, Electronic and Mechanical Engineering, Roma TRE University, Rome, Italy
[1] gabriele.bocchetta@uniroma3.it, [2] giorgia.fiori@uniroma3.it,
[3] andrea.scorza@uniroma3.it, [4] salvatore.sciuto@uniroma3.it

***Abstract* – The high interest of scientists and industries in the application of MEMS micro-actuators to several fields requires effective and robust measurement methods and systems for their quality assessment, focusing on their functional characterization, usually carried out through image analysis-based methods. In this study, a comparison of two experimental setups for image acquisition is proposed, aiming at establishing which setup collects images with higher quality for MEMS microgripper functional evaluation. The proposed work describes an experimental approach based on the evaluation of five parameters, i.e., brightness, saturation, contrast, sharpness, and signal-to-noise ratio, applied to 24 regions of interest in two sets of images of a same micro-actuator acquired from different optical setups at three magnification levels. Measurement results have been assessed following an objective approach by processing the acquired data through an in-house algorithm and a subjective approach by showing the acquired images to six observers and collecting their preferences.**

I. INTRODUCTION

Microgrippers (MGs) are devices based on MEMS (Micro Electro-Mechanical System) technology, able to grasp and manipulate objects of microscopic size, suitable for a wide range of applications, especially in the biomedical field and in particular, the manipulation of cells and tissues where they can contribute to the development of minimally invasive surgery techniques and the characterization of biological samples [1-3]. In this regard, the present study is part of a research aimed at developing image analysis-based measurement methods and systems for the characterization of electrostatic actuated MGs [4-9]. The Device Under Test (DUT) is the MG prototype in Fig. 1, fabricated by Deep Reactive Ion Etching (DRIE) process, using an aluminum hard mask on a silicon-on-insulator wafer [4-5]. Previous studies from the Authors [5-8] focused on measuring the displacement as a function of the supply voltage. Due to the small displacement values obtained for low supply voltage values and the small size of some parts of the device (e.g., the fingers thickness in the comb-drives is 4 µm only), the optical setup should be able to acquire images whose quality guarantee the measurement of a few microns and therefore the performance of a digital imaging system for this type of analysis in optical microscopy strongly depends also on the camera used for image digitalization. In this study, a comparison between two different digital cameras (modified GoPro HERO 10 Black and OrmaEurotek MD6iS) for acquiring images of the microgripper prototype useful for its functional characterization has been carried out.

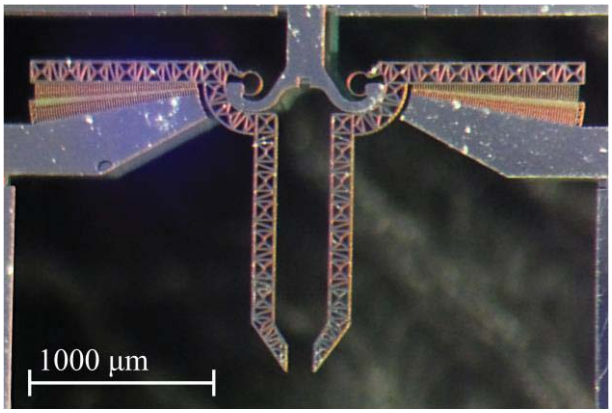

Fig. 1. Front view of the microgripper prototype.

II. MATERIALS AND METHODS

To compare the outcomes from two different optical setups depending on their digital cameras, two sets of images have been acquired under the same operating conditions: illuminance, DUT position, trinocular microscope, lens mount and default camera settings. Three different levels of magnifications have been used on the microscope (16×, 40×, 100×) and from each image, four different square Regions Of Interest (ROIs) have been selected, thus obtaining a total of 24 different ROIs to compare in pairs. In the present work a method for comparing digital cameras in MEMS testing setups is proposed, based on two

different approaches: an objective evaluation, through the use of an in-house software developed in MATLAB, and a subjective approach, showing the different ROIs of the collected images to independent observers. Five representative parameters [9] for the characterization of MEMS micro-actuators have been chosen to carry out the image quality evaluation:

- Brightness – it refers to pixels' intensity and to a visual perception that allows the observer to see an image as lighter or darker. It depends on the energy carried by the electromagnetic waves through the camera sensor and depends on the sensor sensitivity.
- Saturation – it describes the intensity of colors. A high-saturated image is characterized by vivid colors, while a low-saturated one is closer to the grayscale. Saturation, together with brightness, is influenced by the interaction between the DUT and the light source.
- Contrast – it is defined by the difference in luminance between light and dark areas of an image. High contrast makes an object in an image more distinguishable, as for the fingers in the comb-drives.
- Sharpness – it determines the amount of detail a digital camera can reproduce and depends on the acuity between the edges of an object in an image. In a sharp the edges of the DUT are better preserved, e.g., the comb-drive moving part edges, characterized by a triangle-shaped etch-holes pattern, which allow the micro-actuator angular displacement evaluation.
- Signal-to-noise ratio (SNR) – it compares the amount of desired signal to the level of background noise. High SNR values allow appreciating thin parts of the DUT, as in the case of the Conjugate Surfaces Flexural Hinges (CSFH).

Table 1. Experimental Setup

Device	Characteristics
Device Under Test (DUT)	Silicon microgripper prototype equipped with electrostatic rotary comb-drives.
Light Microscope	Zoom Range: 16×, 20×, 40×, 60×, 80×, 100×
Light source	LED Light, Color temperature: 5600 °K
Image Processing Software	In-house algorithm implemented in MATLAB (2021b, MathWorks)
PC	Intel core i7-4790, 32 GB RAM, Nvidia GeForce GTX 960

A. Experimental setup

The DUT is a MG prototype with two electrostatic comb-drive with radial geometry and with two CSFHs. The images of the DUT have been acquired through a trinocular light microscope, equipped with C-mount for the digital camera connection. Furthermore, the microgripper prototype has been placed on an *ad hoc* 3D printed stand to ensure the correct positioning under the microscope. In Table 1, the main components of the experimental setup have been reported.

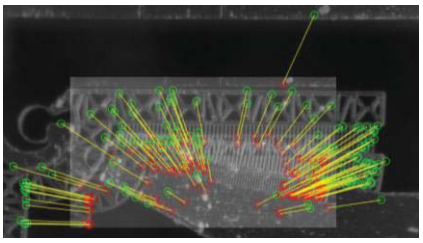

Fig. 2. Matched Kaze Points of Camera A (red) and B (green) images for ROIs transformation evaluation.

B. Comparison among images with different resolution

The acquired images have different sizes, 6.0 MP and 23.3 MP for Camera A and Camera B, respectively and their main specifications have been reported in Table 2, together with the pixel resolution at both minimum and maximum magnification levels, which has been estimated using a micrometric slide. This means that also ROIs have different dimensions for carrying out a comparison [10]. From each image, the Kaze Features [11] have been detected and matched (Fig. 2) in order to find those key points that allow the ROI a transformation [12-13], i.e., a similarity transformation, which is an isometry composed with an isotropic scaling. The algorithm used for the transformation matrix evaluation has been performed for 10^3 cycles for each image pair and the average transformation matrices have been determined.

Table 2. Digital cameras specifications

Specification	Camera A	Camera B
Lens mount	C-mount	C-mount
Number of pixels	6.0 MP	23.3 MP
Sensor model	Sony IMX236	Sony IMX677
Sensor type	CMOS	CMOS
Sensor size	½.8 inch	½.3 inch
Pixel size	2.8 µm	2.0 µm
Image size [pixel]	3264×1840	5568×4176
Pixel resolution at min zoom level (16×) [µm/px]	0.713 ± 0.015	1.060 ± 0.022
Pixel resolution at max zoom level (100×) [µm/px]	0.114 ± 0.004	0.172 ± 0.007

C. Objective image quality assessment

The selected ROIs have been processed and compared in pairs (Fig. 3) and the five parameters have been evaluated using an in-house algorithm implemented in MATLAB. Brightness (*V)* has been assessed as the highest value of a color among the red (*R)*, green (*G)*, and blue (*B)* components, while saturation (*S)* describes the measure of the departure of a hue from achromatic and both have been evaluated following the approach proposed in the HSV hexcone model [14]:

$$V = \max(R,G,B) \qquad S = \frac{V - \min(R,G,B)}{V} \qquad (1,2)$$

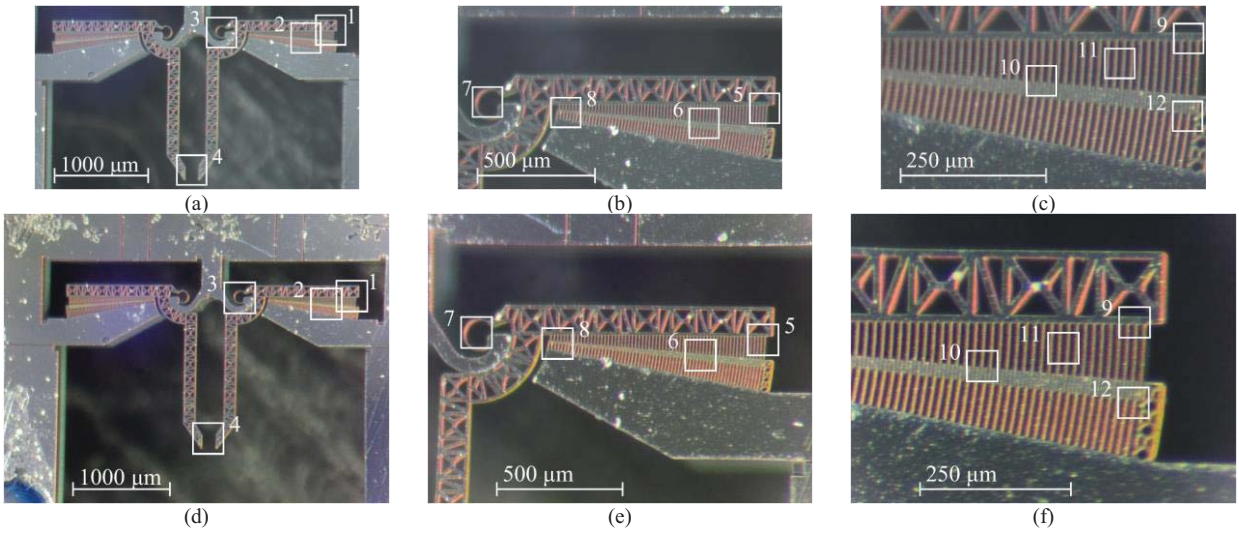

Fig. 3. ROIs in the processed images. Camera A: (a) 16×, (b) 40×, (c) 100×. Camera B: (d) 16×, (e) 40×, (f) 100×.

Contrast (*C*), also defined as the visibility by Michelson in [15], has been calculated following:

$$C = \frac{I_{max} - I_{min}}{I_{max} + I_{min}} \tag{3}$$

where I_{max} and I_{min} represent the highest and lowest luminance, as intensity of the pixels in the grayscale image. Sharpness is a fundamental parameter for evaluating the quality of an image and is an indispensable parameter for measuring small length values in the case of optical microscopy. In scientific literature, several No-Reference methods for sharpness evaluation have been proposed [16-18], most of them based on the maximum gradients and gradients variability, the calculation of the width of edges, modulation transfer function (MTF) and Spatial Frequency Response (SFR). This is due to the fact that although the human eye is easily able to distinguish sharp from blurred areas in an image, to present day, it is yet laborious for numeric computing environments. In the present work, sharpness evaluation algorithm is based on Local Phase Coherence (LPC) analysis. This parameter has been proposed in [19-20], in which it has been shown that a local phase variation is a more important factor than high-frequency energy for sharpness perception. Specifically, defined edges cause a solid coherence in local phase in the complex wavelet transform domain. For the SNR evaluation, the acquired images of the microgripper prototype have been compared with two sets of images by keeping the microscope in the same position, but without the DUT (considered as the desired signal) positioned on the 3D printed stand. Following [21], the SNR has been evaluated pixel by pixel as:

$$SNR = I / I_B \tag{4}$$

where I_B represents the background image, considered as noise. Finally, the proportion between the number of pixels characterized by a SNR greater than a threshold value to the number of ROI total pixels has been calculated.

D. Subjective image quality assessment

A subjective score is of utmost importance in imaging system quality evaluation, particularly in the case of biomedical imaging systems [18,21-24]. In literature comparisons of different methods for subjective images quality assessment have been presented, and among them, the forced-choice pairwise comparison has been found to be the most accurate [25], and besides, it has also been reported as the easiest for observers, as it requires a direct comparison between two images shown simultaneously and only one choice. Therefore, the proposed subjective approach is based on the forced-choice pairwise comparison method, showing all selected ROIs in pairs, in random order, to six independent observers, who have been asked to choose which of the two ROIs presented the higher value of each of the five parameters.

Table 3. Variable settings in MCS

Parameter	Distribution	Camera A		Camera B	
		μ_A	σ_A	μ_B	σ_B
ROI size [px]	Uniform	300	15	446	23
ROI shift [px]	Uniform	0	15	0	23

III. RESULTS AND DISCUSSION

In this section, the preliminary results obtained by means of the two different setups have been reported and commented. Before discussing the results, a Monte Carlo Simulation (MCS) with 10^4 iterations has been carried out to evaluate the software uncertainty, since the ROIs position depends directly on the operator's decision and because of pixel approximations in the transformation matrix evaluation. The following uniform distributions, shown in Table 3, have been assigned to the variables influencing the present study: ROI size and ROI shift, expressed as number of pixels. Moreover, for Camera A and B images, the standard deviation values (σ_A and σ_B)

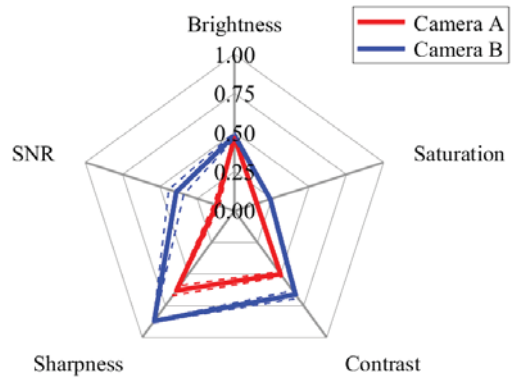

Fig. 4. Example of the Kiviat diagram applied to the objective image quality assessment results.

have been assumed as 5% of the corresponding ROIs average size (μ_A and μ_B respectively). The uncertainty has been expressed following Chebyshev's inequality [26], as three times the value of the calculated standard deviation. In order to express an overall score describing the two digital cameras, ROIs enclosing the same MG part for every image at each level of magnification have been considered, and in particular those ROIs representing the comb-drive fingers that are the useful elements for the displacement evaluation. The obtained parameters have been plotted on a Kiviat diagram, shown in Fig. 4, and the polygon with the largest area represents the digital camera with the highest total score and consequently the digital camera that is able to acquire microgripper images with higher quality. Table 4 shows the results obtained by the objective and the subjective method, with their relative uncertainties. The total scores evaluated by the image quality assessment algorithm are 0.28 ± 0.04 and 0.65 ± 0.07 for Camera A and Camera B respectively. As regards the subjective method, each one of the six observers repeated the test six times and the obtained results have been computed as the average of all individual tests and they have been expressed with a maximum score of 6, while the uncertainty has been evaluated with the Square-

Table 4. Experimental results

Parameter	Camera A	Camera B
	Objective image quality assessment	
Brightness	0.47 ± 0.01	0.48 ± 0.02
Saturation	0.15 ± 0.01	0.24 ± 0.01
Contrast	0.50 ± 0.02	0.66 ± 0.03
Sharpness	0.63 ± 0.04	0.87 ± 0.01
SNR	0.12 ± 0.02	0.39 ± 0.05
Total score	**0.28 ± 0.04**	**0.65 ± 0.07**
	Subjective image quality assessment	
Brightness	1.1 ± 1.0	4.9 ± 2.2
Saturation	0.1 ± 0.3	5.9 ± 2.4
Contrast	0.5 ± 0.7	5.5 ± 2.4
Sharpness	1.1 ± 1.1	4.9 ± 2.2
SNR	0.9 ± 0.9	5.1 ± 2.3

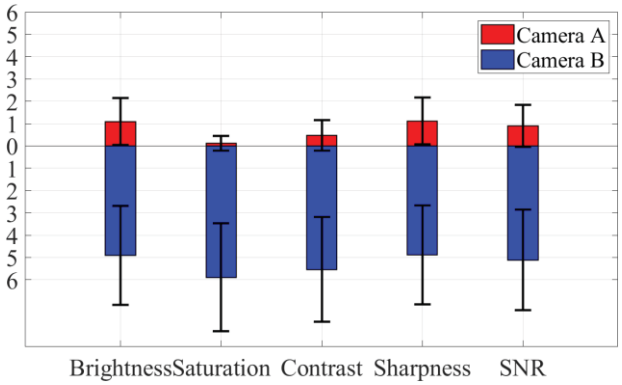

Fig. 5. Subjective image quality assessment results.

Root Rule for Counting Experiments, following the approach in [27]. Finally, the subjective image quality assessment scores have been evaluated by combining the results obtained from all the observers and as shown in Fig. 5 Camera B scored higher values for each considered parameter, thus supporting the objective image quality assessment results, and demonstrating that for both methods it is able to capture images with higher quality for MEMS actuators functional assessment.

IV. CONCLUSIONS

The present preliminary study aims at comparing 24 different ROIs to determine the higher image quality to identify which of two different cameras is most suitable to be integrated into an optical setup for the analysis of the MEMS micro-actuators characteristics. Five parameters (brightness, saturation, contrast, sharpness and SNR) have been evaluated for every region of interest, following both an objective and a subjective approach. Two sets of images of a MG prototype for three different levels of magnification have been acquired through a trinocular optical microscope equipped with two different digital cameras. The acquired images have been processed through an image quality assessment algorithm implemented by the Authors. The uncertainty analysis of the method has been carried out through a Monte Carlo Simulation with 10^4 iterations. The obtained results of this preliminary study confirm that Camera B images are characterized by higher quality: higher values of contrast, sharpness and SNR allow a better determination of the parts that compose the micro-actuator, useful for the functional characterization. Moreover, Camera B is equipped with a larger sensor and a higher resolution that ensure the acquisition of a larger area and a higher micron/pixel ratio, respectively. In the near future, it will be important to improve the experimental setup and the image processing algorithm, to perform further tests and comparisons between the two digital cameras focusing on other aspects for the MG prototype characterization, such as the video quality assessment, especially if the prototype behavior over time is going to be studied, e.g., if the MG is supplied with a periodic signal.

REFERENCES

[1] K.R.Oldham, “Applications of MEMS technologies for minimally invasive medical procedures”, in “MEMS for Biomedical Applications”, Woodhead Publishing, 2012, pp. 269–290.

[2] S.Byun, J.-M.Lim, S.-J.Paik, A.Lee, S.Park, J.Park, “Barbed micro-spikes for micro-scale biopsy”, J. Micromech. Microeng., vol.15, No.6, May 2005, pp. 1279–1284.

[3] M.Verotti, P.Di Giamberardino, N.P.Belfiore, O.Giannini, “A genetic algorithm-based method for the mechanical characterization of biosamples using a MEMS microgripper: numerical simulations”, J. Mech. Behav. Biomed. Mater., vol.96, August 2018, pp. 88–95.

[4] A.Bagolini, S.Ronchin, P.Bellutti, M.Chistè, M.Verotti, N.P.Belfiore, “Fabrication of Novel MEMS Microgrippers by Deep Reactive Ion Etching with Metal Hard Mask”, J. Microelectromechanical Syst., vol.26, No.4, May 2017, pp. 926–934.

[5] N.P.Belfiore, A.Bagolini, A.Rossi, G.Bocchetta, F.Vurchio, R.Crescenzi, A.Scorza, P.Bellutti, S.A.Sciuto, “Design, Fabrication, Testing and Simulation of a Rotary Double Comb Drives Actuated Microgripper”, Micromachines, vol.12, No.10, October 2021, p. 1263.

[6] F.Vurchio, G.Bocchetta, G.Fiori, A.Scorza, N.P.Belfiore, S.A.Sciuto, “A preliminary study on the dynamic characterization of a MEMS microgripper for biomedical applications,” Proc. of 2021 IEEE International Symposium on Medical Measurements and Applications (MeMeA), 2021.

[7] F.Vurchio, G.Fiori, A.Scorza, S.A.Sciuto, “A comparison among three different image analysis methods for the displacement measurement in a novel MEMS device,” Proc. of 24th IMEKO TC4 International Symposium and 22nd International Workshop on ADC and DAC Modelling and Testing, 2020, pp. 327–331.

[8] F.Vurchio, P.Ursi, F.Orsini, A.Scorza, R.Crescenzi, S.A.Sciuto, N.P.Belfiore, “Toward operations in a surgical scenario: Characterization of a microgripper via light microscopy approach”, Appl. Sci., vol.9, No.9, May 2019.

[9] R.C.Gonzalez, R.E.Woods, “Digital Image Processing”, 4th Edition, Pearson, 2018.

[10] Y.Dufournaud, C.Schmid, R.Horaud, “Image matching with scale adjustment”, Comput. Vis. Image Underst., vol.93, No. 2, February 2004, pp. 175–194.

[11] P.F.Alcantarilla, A.Bartoli, A.J.Davison, “KAZE Features,” Proc. of ECCV 2012, pp. 214–227.

[12] M.Muja, D.G.Lowe, “Fast Matching of Binary Features,” Proc. of Conference on Computer and Robot Vision. CRV, 2012.

[13] R.Hartley, A.Zisserman, “Multiple View Geometry in Computer Vision”, 2nd ed. Cambridge, UK; New York: Cambridge University Press, 2003.

[14] A.R.Smith, “Color gamut transform pairs,” Proc. of 5th Annual Conference on Computer Graphics and Interactive Techniques (SIGGRAPH ‘78), 1978, pp. 12–19.

[15] A.Michelson, “Studies in Optics”, University of Chicago Press, 1927.

[16] Y.Zhan, R.Zhang, “No-Reference Image Sharpness Assessment Based on Maximum Gradient and Variability of Gradients”, IEEE Trans. Multimed., Vol.20, No.7, July 2018, pp. 1796–1808.

[17] K.Bahrami, A.C.Kot, “A fast approach for no-reference image sharpness assessment based on maximum local variation”, IEEE Signal Process. Lett., vol.21, No.6, June 2014, pp. 751–755.

[18] M.Ukishima, T.Nakaguchi, K.Kato, Y.Fukuchi, N.Tsumura, et al., “Sharpness comparison method for various medical imaging systems”, IEICE Trans. Inf. Syst., Vol.J89-A, No.11, 2006, pp.914–921.

[19] R.Hassen, Z.Wang, M.M.A.Salama, “Image sharpness assessment based on local phase coherence”, IEEE Trans. Image Process., vol.22, No.7 , July 2013, pp. 2798–2810.

[20] S.Ryu, K.Sohn, “No-reference sharpness metric based on inherent sharpness”, Electron. Lett., Vol.47, No.21, November 2011, pp. 1178–1180.

[21] G.Fiori, F.Fuiano, A.Scorza, J.Galo, S.Conforto, S.A.Sciuto, “A Preliminary Study on the Adaptive SNR Threshold Method for Depth of Penetration Measurements in Diagnostic Ultrasounds”, Appl. Sci., vol.10, No.18, September 2020, 6533.

[22] G.Fiori, F.Fuiano, A.Scorza, J.Galo, S.Conforto, S.A.Sciuto, “A preliminary study on an image analysis based method for lowest detectable signal measurements in PW Doppler ultrasounds”, ACTA IMEKO, vol.10, No.2, June 2021, pp.126–132.

[23] S.Koho, E.Fazeli, J.E.Eriksson, P.E.Hänninen, “Image Quality Ranking Method for Microscopy”, Sci. Rep., vol.6, August 2016, pp. 1–15.

[24] C.Otero, N.García-Porta, et al., “Comparison of different smartphone cameras to evaluate conjunctival hyperaemia in normal subjects”, Sci. Rep., vol.9, No.1, February 2019, pp. 1–8.

[25] R.K.Mantiuk, A.Tomaszewska, R.Mantiuk, “Comparison of Four Subjective Methods for Image Quality Assessment”, Comput. Graph. Forum, vol.31, No.8, December 2012, pp. 2478–2491.

[26] W.C.Navidi, “Statistics for Engineers and Scientists”, 5th edition, McGraw-Hill Education, New York, USA, 2020.

[27] J.R.Taylor, “An introduction to Error Analysis: The study of Uncertainties in Physical Measurements”, 2nd edition, University Science Books, New York, USA, 1997.